Microelectronics Reliability xxx (2017) xxx–xxx

Contents lists available at ScienceDirect

Microelectronics Reliability

journal homepage: www.elsevier.com/locate/microrel

Thermal state of electronic assemblies applied to smart building equipped with QFN64 device subjected to natural convection

A. Baïri [a,*], L. Roseiro [b], A. Martín-Garín [c], K. Adeyeye [d], J.A. Millán-García [c]

[a] University of Paris, LTIE-GTE EA 4415, 50, rue de Sèvres, F-92410 Ville d'Avray, France
[b] Polytechnic Institute of Coimbra, ISEC, DEM, Rua Pedro Nunes, Quinta da Nora, 3030-199 Coimbra, Portugal
[c] University of the Basque Country, ENEDI Research Group, Plaza Europa 1, E-20018 San Sebastián, Spain
[d] University of Bath, Department of Architecture and Civil Engineering, Claverton Down, Bath BA2 7AY, UK

ARTICLE INFO

Article history:
Received 4 October 2016
Received in revised form 25 December 2016
Accepted 6 January 2017
Available online xxxx

Keywords:
Thermal control
Free convection
Smart building, Home automation, Architecture
Water consumption control
Quad flat non-lead (QFN64) electronic device
Electronics reliability
Experience and CFD

ABSTRACT

The performance and reliability of electronic components and assemblies strongly depend on their thermal state. The knowledge of the temperature distribution throughout the assembly is therefore an essential element to ensure their correct operation. This is the main objective of this work that examines the case of a conventional assembly equipped with a quad flat non-lead QFN64 subjected to free convection. This active electronic package is welded on a PCB which may be inclined by an angle varying between 0° and 90° (horizontal and vertical positions respectively) and generates during its operation a high power ranging from 0.1 to 1 W. Thermoregulation of the assembly is ensured by natural convection, given its many well known advantages in this engineering field. Accurate relationships are proposed to determine the temperature on different areas of the device and the PCB. They are determined by means of a 3D numerical approach based on the finite volume method confirmed by measurements on an actual installation. These relationships allow reliability improvement of these electronic assemblies that are widely used in many engineering fields such as computing industry, mobile telephony, home automation, automotive, embarked electronics and the smart building applications considered in this work. The present survey complements a recent study which quantifies the natural convective heat transfer on the considered electronic assembly equipped with the QFN64 device, for the same power range and angle of inclination.

1. Introduction

The performance and reliability of electronic components and assemblies strongly depend on their thermal state and characteristics [1–3]. In electronics, natural convection is the preferred heat transfer mode, given its numerous advantages. It avoids the inconvenience of the forced convection which requires implementation of mechanisms such as fans that generate noise and electromagnetic pollution, need power supply and can potentially break down. This reduces the reliability of the assembly and it can be prohibited in some engineering areas which requires high performance. The heat transfer phenomena and particularly natural convection in closed cavities depends on many physical parameters [4–8]. The natural convective flow and heat transfer between the electronic assembly and its environment is influenced by the geometry and dimensions of the assembly, as well as those of the enclosure containing it. The power generated by the heat sources (active components), their position in the assembly, their inclination relative to the gravitational field, as well as temperature levels and thermal characteristics of the fluid are among the other most infuential parameters. The well-known quad flat non-lead (QFN) devices are examined in the present work and detailed in various documents [9–10]. Different aspects of these devices were also examined to improve their integration in the industrial assemblies [11–14]. The assemblies containing these devices requires precise knowledge of the convective heat transfer coefficient on all of the assembly's surfaces. This has been recently done for the devices with 16, 32 and 64 leads denoted QFN16 [15], QFN32 [16] and QFN64 [17] respectively. These active packages are welded on a printed circuit board (PCB) inclined with respect to the horizontal plane at an angle varying between 0° and 90°. Many generated power ranges (low and high ranges) varying between 0.01 and 1.0 W are considered. For these electronic assemblies, it is clearly shown [18] that the thermal conductivity of the upper copper layer of the PCB highly affects the thermal behaviour of the electronic assemblies. The results are presented by means of specific relationships. The overall heat transfer coefficient of the low powered QFN64 model was determined [19] for some values of the generated power ranging from 0.01 to 0.1 W. The temperature distribution in the electronic assemblies must be controlled to check that the maximum value recommended by the manufacturers of the electronic equipment is not reached or exceeded, to avoid its malfunction and in some cases its destruction.

* Corresponding author at: University of Paris, Laboratoire Thermique Interfaces Environnement, LTIE-GTE EA 4415, 50 rue de Sèvres, F-92410 Ville d'Avray, France.
E-mail addresses: bairi.a@gmail.com, abairi@u-paris10.fr (A. Baïri).

http://dx.doi.org/10.1016/j.microrel.2017.01.002
0026-2714/

Nomenclature

A_i	surface of a given i area (m^2)
g	gravity acceleration ($m\ s^{-2}$)
$\overline{h}_i$	average convective heat transfer coefficient of a given i area ($Wm^{-2}\ K^{-1}$)
P	generated power (W)
P_i	convective heat power exchanged by a given i area (W)
$\overline{T}_i$	calculated average temperature of a given i area (K)
$\overline{T_m}$	measured average temperature (K)
T_c	temperature of the cavity's walls; initial temperature of the whole system (°C)

Greek symbols

α	inclination angle of the PCB with respect to the horizontal plane (°)
$\Delta\overline{T}$	calculated temperature difference; $\Delta\overline{T} = (\overline{T} - T_c)$ (K)
$\Delta\overline{T_m}$	measured temperature difference; $\Delta\overline{T_m} = (\overline{T_m} - T_c)$ (K)
$\Delta\overline{T_m}_{max}$	maximum $\Delta\overline{T_m}$ value (K)
$\Delta\overline{T_m^*}$	ratio defined by $\Delta\overline{T_m^*} = \Delta\overline{T_m}/\Delta\overline{T_m}_{max}$ (-)
λ_a	air thermal conductivity ($Wm^{-1}\ K^{-1}$)
λ	thermal conductivity of the materials ($Wm^{-1}\ K^{-1}$)

This applies to the passive parts as the Printed Circuit Board (PCB) which support components, in order to avoid the separation of the copper layer from the substrate (epoxy resin) or desoldering the components. The junction temperature of the QFN64 device considered in the present work must be maintained below a maximal value recommended by the manufacturers. This criterion has to be respected under the most unfavorable thermal and geometric conditions. The thermal design and management of the electronic assemblies are highly dependent on several physical parameters and the environment in which they are installed [20–21]. The effects of the molding compound on the QFN64's maximal temperature has been quantified in the survey [22] which shows that the material used to encapsulate the package significantly affects its thermal behaviour during operation. The thermal sizing of these electronic assemblies requires also the knowledge of the temperature distribution on all the surfaces of the assembly.

The present work discusses the case of an electronic assembly equipped with a QFN64 device, used in home automation and smart building for simultaneous control of various equipment such as windows, boilers, air conditioning systems, lighting, and water consumption. The QFN64 is welded on a PCB installed in an air-filled cavity. The board can be inclined relatively to the horizontal at an angle varying between 0° and 90° (horizontal and vertical positions respectively) by steps of 15°. During operation, the QFN64 generates a high power ranging from 0.1 to 1 W. The average temperature corresponding to every area of this electronic assembly can be determined by means of relationships proposed in this survey according to the generated power and the package tilting angle. These relationships determined by means of 3D numerical work based on the finite volume method are confirmed by measurements on an actual installation. They help to improve the reliability of these electronic assemblies widely used in many engineering applications. This study complements the current knowledge concerning this important component, available in the specialized literature and examined in various companies [23].

2. The considered assembly

The parallelepipedic QFN64 package (9 mm × 9 mm × 1 mm, Fig. 1(a)) considered in this survey is welded on a rectangular single face PCB (30 mm × 13 mm; 1.6 mm epoxy + 35 μm copper layer) Fig. 1(b)). The board could be inclined with respect to the horizontal plane by an angle α varying between 0° and 90° (Fig. 1(c)). The top face, the sides and the back face of the QFN device are denoted as (Q_T), (Q_S) and (Q_B) respectively.

The PCB is decomposed into three distinct areas denoted as (B_T), (B_S) and (B_B) respectively representing its top, sides and back faces respectively. The assembly is installed in an air-filled parallelepipedic cavity (35 mm × 20 mm × 8 mm) whose walls are maintained isothermal at temperature $T_c = 293.15K$. The thermal conductivity λ of the materials constituting the assembly are of 120, 260, 260, 2.1, 0.66 for the die, the diepad, the leads, the paste and the molding compound (resin) respectively. These values have been measured within ±3% by means of the Hot Disk TPS 2500 model [24], based on the transient plane source (TPS) method [25], with parallelepipedic samples (square side 12 mm, 4 mm thick) provided by a QFN's manufacturer. The copper network density corresponds to a Copper ratio of 5.26% (see [18]). The resulting thermal conductivity of the PCB according to its plane is of 20 $Wm^{-1}\ K^{-1}$ and 0.35 in its thickness. This important aspect has been treated in previous works as [26].

3. Numerical procedure

Calculations are processed for the (Q_T), (Q_S), (B_T), (B_S) and (B_B) areas by means of a 3D numerical survey based on the finite volume method. Details of the calculating procedure are available in [17]. To simplify the presentation of the results in the continuation of this work, the two surfaces (B_S) and (B_B) are grouped as ($B_B + B_S$). Furthermore, an fictitious surface denoted as (Q_B) is designed to facilitate the direct modeling of the package without the PCB. However, the results concerning this area take into account the convective heat transfer that occur on the PCB. They were obtained by means of a thermal balance performed on the entire assembly. The temperature gradient $(\partial T/\partial n)_k$ concerning any k element of the surface all around the assembly determines the corresponding local convective heat transfer coefficient $h_k = [-\lambda_a(\partial T/\partial n)/(T - T_c)]_k$ whose integration weighted by the surfaces S_k allows determination of the average convective heat transfer coefficient $\overline{h}_i = (\sum_k h_k S_k)/(\sum_k S_k)$ concerning a given i area. Its association with the power P_i exchanged by convection provides then the average difference temperature $\overline{T}_i$ of every area by means of the Newton's law $P_i = \overline{h}_i A_i(\overline{T}_i - T_c)$, being A_i the surface of the considered i area. This operation was performed for all the configurations obtained by varying the high power generated by the QFN64 between 0.1 and 1.0 W, and the tilt angle α between 0° and 90° by steps of 15°.

Evolution of the temperature difference $\Delta\overline{T} = \overline{T} - T_c$ presented in Figs. 2 and 3 versus α and P respectively shows that $\Delta\overline{T}$ decreases as the PCB inclination angle increases between the horizontal position ($\alpha = 0°$) and the vertical one ($\alpha = 90°$), on all areas.

The decrease is however less significant on (Q_B). The change is more pronounced for large P values, almost zero for the lowest value ($P = 0.1W$). The highest values of $\Delta\overline{T}$ are observed on the QFN sides (Q_S). In this region, the conductive resistance is greater according to the reduced exchange surface. Fig. 3 shows a significant $\Delta\overline{T}$ difference between (Q_S) and (Q_T). The lowest values of the mean temperature concern the PCB which acts as a fin. The heating of the board is limited to the immediate vicinity of the device, the rest being almost at the environment temperature.

4. Experimental approach

Experimental measurements were performed with the assembly presented in Fig. 1(d) to check the numerical results. The QFN64 (1 in Fig. 1(d)) is welded on a rectangular (30 mm × 13 mm) single side conventional PCB (35 μm of copper on an 1.6 mm width epoxy base, (2 in Fig. 1(d)). The device is connected to the other components of the

Please cite this article as: A. Baïri, et al., Thermal state of electronic assemblies applied to smart building equipped with QFN64 device subjected to natural convection, Microelectronics Reliability (2017), http://dx.doi.org/10.1016/j.microrel.2017.01.002

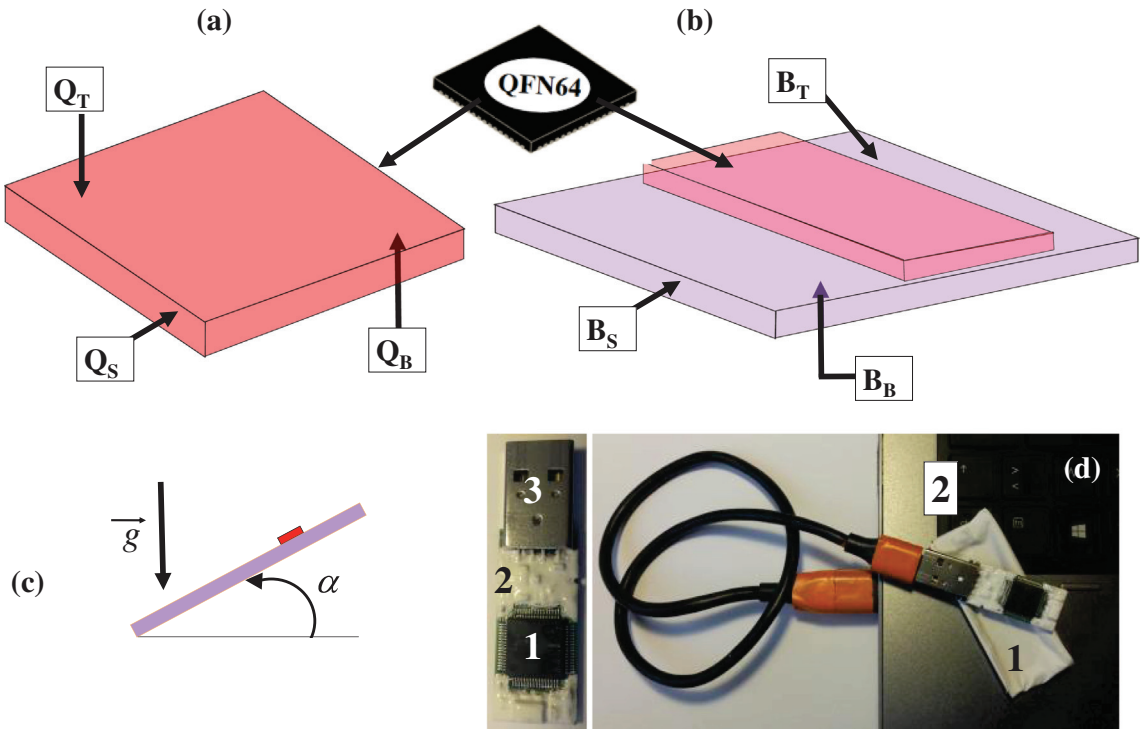

Fig. 1. (a) The considered QFN64 with its (Q_T), (Q_S) and (Q_B) areas; (b) The PCB with its (B_T), (B_S) and (B_B) areas; (c) the PCB inclination angle α; (d) The considered assembly.

assembly by a standard copper network. The board is linked to a USB type plug (3, Fig. 1(d)) which is used to power-on the QFN and to measure all the electronic assembly parameters. The assembly is installed in the center of a parallelepipedic box (35 mm long × 20 mm wide × 8 mm thick; (1) in Fig. 1 (d)). The USB plug is connected to a computer (2, Fig. 1(d)) equipped with a fast data acquisition system and a conventional resistor assembly including a resistance calibrated previously. An internal multimeter-multiplexer of high resolution (3×10^6 points) allows the measurement of the intensity of the current I and U voltage of the device's active source with an accuracy of 0.1% and 0.08% respectively in the ranges concerned by the tests. The power generated by the $P = UI$ is so determined with a maximum error of 0.2% ($\Delta P/P = \Delta U/U + \Delta I/I \approx 0.2\%$).

The thermal state of the whole system is measured by means of 24 K-type calibrated thermocouples of 0.04 mm diameter. They are welded by laser technique on the surfaces of assembly: 5 on the diagonals of (Q_T)

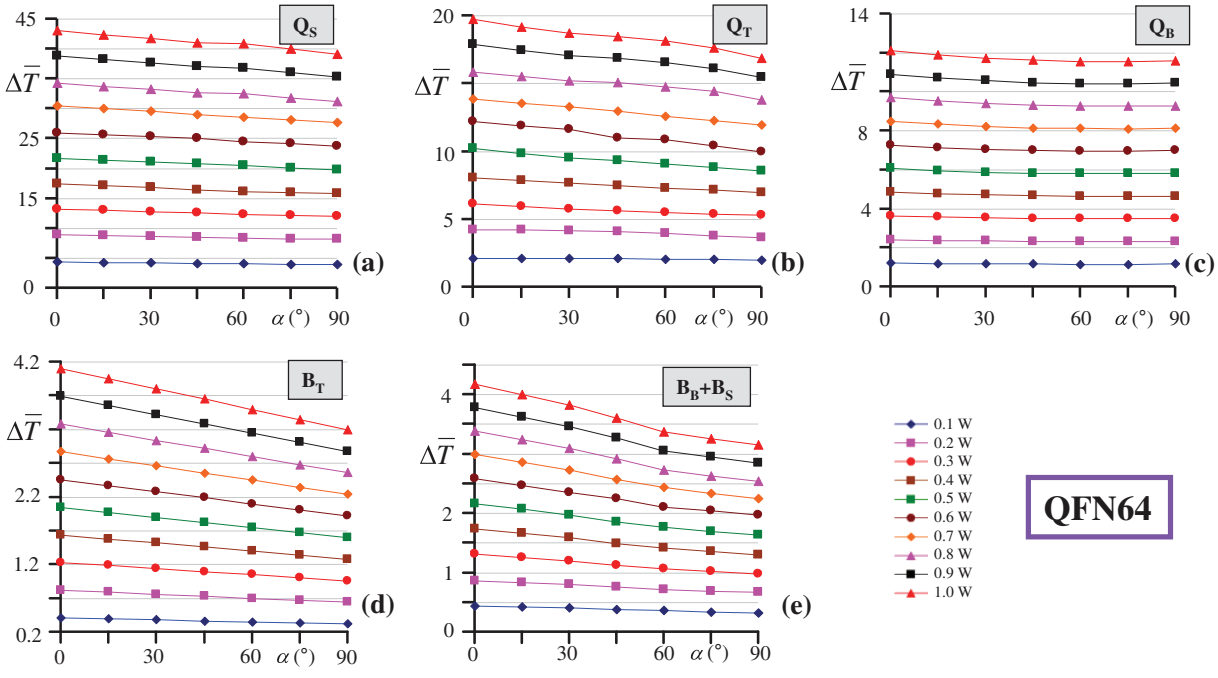

Fig. 2. Evolution of $\Delta\overline{T}$ versus α on (Q_T), (Q_S), (Q_B), (B_T) and ($B_B + B_S$) areas.

Please cite this article as: A. Baïri, et al., Thermal state of electronic assemblies applied to smart building equipped with QFN64 device subjected to natural convection, Microelectronics Reliability (2017), http://dx.doi.org/10.1016/j.microrel.2017.01.002

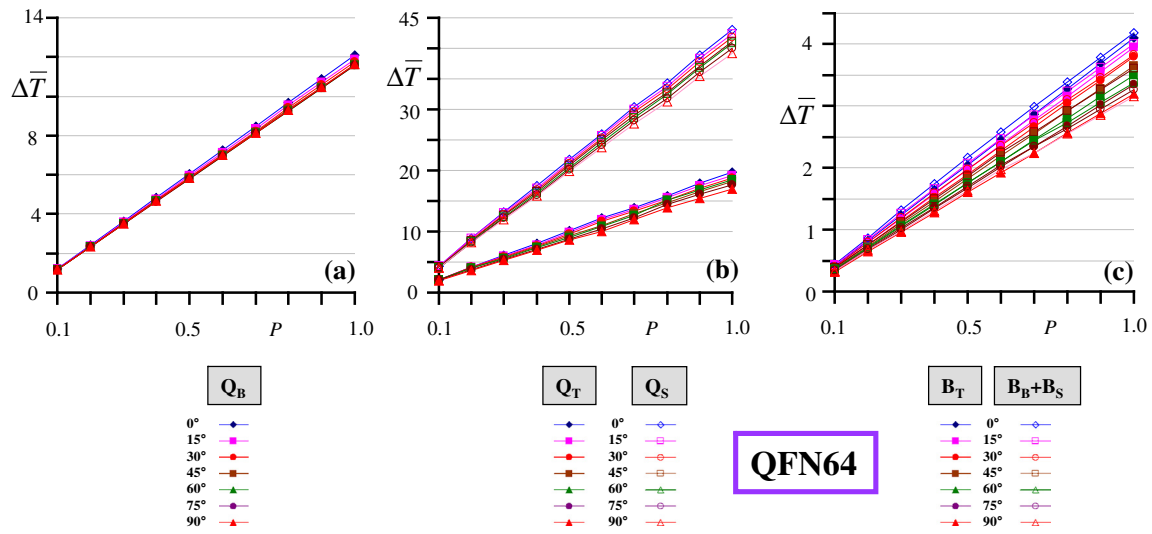

Fig. 3. Evolution of $\Delta\overline{T}$ versus P on (Q_T), (Q_S), (Q_B), (B_T) and (B_B+B_S) areas. High powered QFN64 package $(0.1 \le P \le 1.0W)$.

and (Q_B), 1 on each of the 4 (Q_S) sides, 4 on the center axis of (B_T) and 6 on the center axis of (B_B). Thermocouples are welded simultaneously with the other components of the assembly to avoid wire tangling. They are connected to specific plugs located on the back area (B_B) electrically insulating, and communicate with the mother card which is connected to the computer. The 5 thermocouples of (Q_T) are protected by a 10 μm resin layer deposited with the pressurized spray technique. The temperature uncertainty is estimated at $\pm 0.5\%$ in the considered thermal range, following an in-situ calibration. The electronic assembly inclined to the angle α considered for the test is installed in a room whose temperature is maintained at temperature $T_c(\pm 0.1\ K)$. All the measurements (temperatures and electrical data) are made at steady state with a sampling time of 100 ms. The measurements are taken for 10 min after the start of the steady-state regime which is characterized by a relative variance for all temperatures less than 0.3%. The average measured temperature difference $\Delta\overline{T_m} = (\overline{T_m} - T_c)$ for each area is determined with the average value of the measured temperatures weighted by the corresponding surfaces. Direct measurement of the temperature difference allows limiting the uncertainty measurement of the thermal state to $\pm 0.5\%$. All combinations of $0.1 \le P \le 1.0W$ step 0.1W with $0 \le \alpha \le 90°$ step 15° were tested.

Comparison between measured $\Delta\overline{T_m}$ and calculated $\Delta\overline{T}$ temperature differences for $\alpha = 0$ and 90° on (Q_T) and (Q_S) areas shows a very good agreement: 3% and 4% for the average and maximum deviation respectively.

The comparison experience-calculation presented in Fig. 4(a) for $\alpha = 0$ and 90° on (Q_T) and (Q_S) areas illustrates the low deviation and confirms the validity of the calculated values. Furthermore, an IR thermography of the assembly was made by means of a high-resolution infrared camera (Flir Systems ThermoVision A40M type) equipped with a Focal Plane Array detector [27]. Calibration of the overall assembly was made with a Class 1 black body. The Fig. 4(b) presents the distribution of the dimensionless temperature difference $\Delta\overline{T_m^*} = \Delta\overline{T_m}/\Delta\overline{T_{m\max}}$ on the upper face of the QFN64 for the combination $(\alpha = 0, P = 0.5W)$, $\Delta\overline{T_{m\max}}$ being the maximum $\Delta\overline{T_m}$ value corresponding to a given generated power.

Many tests were also performed in order to check the reliability, durability, aging and robustness of the assembly. Several cycles of powering up and disconnection of the package have been carried out, thus subjecting it to variable thermal stresses. The tests done according to the envisaged applications were carried out for many $(0 \le \alpha \le 90°, 0.1 \le P \le 1.0W)$

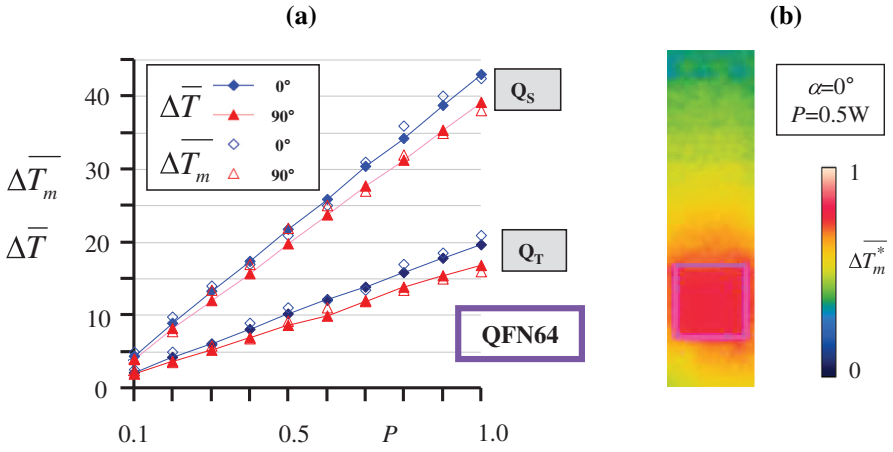

Fig. 4. (a) Comparison between measured $\Delta\overline{T_m}$ and calculated $\Delta\overline{T}$ temperatures on (Q_T) and (Q_S) areas, for $\alpha = 0$ and 90° (b) distribution of $\Delta\overline{T_m^*} = \Delta\overline{T_m}/\Delta\overline{T_{m\max}}$ on the upper face of the assembly for $(\alpha = 0, P = 0.5W)$.

Please cite this article as: A. Baïri, et al., Thermal state of electronic assemblies applied to smart building equipped with QFN64 device subjected to natural convection, Microelectronics Reliability (2017), http://dx.doi.org/10.1016/j.microrel.2017.01.002

combinations. The results of the tests are satisfactory, ascertained by reproducible, consistent and stable responses of the assembly.

5. Relationships

The least squares optimization technique was used to develop relationships allowing calculation of the average temperature difference $\Delta\overline{T}$ of all the assembly's areas according to the generated power P and inclination angle α. In a first step, the optimization has quantified the influence of α on $\Delta\overline{T}$ by means of correlations minimizing the sum of squared residuals between the value calculated with the numerical approach and the fitted value obtained with the function which best models evolution of $\Delta\overline{T}$ versus α. The same work was done in a second step to determine the influence of P on $\Delta\overline{T}$, by using the results obtained in the first step. Both steps are based on a coefficient of determination greater than 0.998.

Finally, the average temperature difference can be calculated in any area of the assembly by means of the following relationships of $(\Delta\overline{T}_i - P - \alpha)$ type.

$$\begin{bmatrix} \Delta\overline{T}_{Q_T} = (19.5-0.031\alpha)P + 0.2 \\ \Delta\overline{T}_{Q_S} = (42.9-0.042\alpha)P + 0.2 \\ \Delta\overline{T}_{Q_B} = \left(12.4-0.017\alpha + 1x10^{-4}\alpha^2\right)P \\ \Delta\overline{T}_{B_T} = (4.07-0.01\alpha)P \\ \Delta\overline{T}_{(B_B+B_S)} = (4.2-0.013\alpha)P \end{bmatrix} \quad (1)$$

$$\text{Valid for} \begin{cases} \text{QFN64} \\ 0 \le \alpha \le 90\ ^\circ \\ 0.1 \le P \le 1\text{W} \end{cases}$$

The associated coefficient of determination are higher than 0.998, which confirms their validity. They allow sizing the QFN64 device, while controlling its temperature according to manufacturers' recommendations.

6. Discussion and conclusion

The results of this numerical and experimental work clearly confirm different temperatures on every area of the considered electronic assembly equipped with QFN64. The influence of the power generated by this device and its inclination relative to the gravitational field on the surface temperature is highlighted. The part of power generated by the source is predominantly (around 94%) exchanged by natural convection through its back face. The results clearly show that on all the areas of the considered electronic assembly, the surface temperature decreases as the PCB inclination angle increases from the horizontal to the vertical position. This trend is more pronounced for the large powers generated by the device. The study also shows that the PCB is the coldest part of the assembly, and that the maximum average surface temperature is observed on the QFN sides, which is due to a high conductive resistance. These observations are useful for the thermal design of these assemblies. The relationships proposed in this work facilitate the calculation of the average temperature on each surface. They can be applied in different engineering fields such smart buildings and home automation, the focus of the current work. They constitute an important tool for the thermal design of these electronic assemblies, to increase their reliability and contribute to improving their performance. The present paper complements a recent study which quantifies the natural convective heat transfer on the considered electronic assembly equipped with the QFN64 device, for the same power range and angle of inclination.

References

[1] D. Vasileska, K. Raleva, Special issue, electrothermal and thermoelectric modeling of nanoscale devices, J. Comput. Electron. 15 (1) (2016) 1–346.
[2] T. Saenen, T.M. Baelmans, Size effects of a portable two-phase electronics cooling loop, Appl. Therm. Eng. 50 (1) (2013) 1174–1185.
[3] M.R. Narayanan, H.D. Al-Nashash, M. Chandra, Thermal model of MOSFET with SELBOX structure, J. Comput. Electron. 12 (4) (2013) 803–811.
[4] T. Basak, R. Anandalakshmi, S. Roy, I. Pop, Role of entropy generation on thermal management due to thermal convection in porous trapezoidal enclosures with isothermal and non-isothermal heating of wall, Int. J. Heat Mass Transf. 67 (2013) 810–828.
[5] M.M. Rashidi, S. Abelman, N.F. Mehr, Entropy generation in steady MHD flow due to a rotating porous disk in a nanofluid, Int. J. Heat Mass Transf. 62 (2013) 515–525.
[6] E. Abu-Nada, Dissipative particle dynamics simulation of natural convection using variable thermal properties, Int. Commun. Heat Mass Transfer 69 (2015) 84–93.
[7] M.A. Sheremet, H.F. Oztop, I. Pop, MHD natural convection in an inclined wavy cavity with corner heater filled with a nanofluid, J. Magn. Magn. Mater. 416 (2016) 37–47.
[8] N. Chen, K. Chiang, T.D. Her, Y.L. Lai, C. Che, Electrical characterization and structure investigation of quad flat non-lead package for RFIC applications, Solid State Electron. 47 (2003) 315–322.
[9] Guidelines for Reporting and Using Electronic Package Thermal Information, Jedec Solid State Technology Association, 2005 (JESD51-12).
[10] Assembly Guidelines for QFN (Quad Flat No-lead) and DFN (Dual Flat No-lead) Packages, Freescale Semiconductor, Inc., Application Note, Document Number: AN1902, Rev. 7.0, 10/2014.
[11] L. Xu, Y. Liu, S. Liu, Modeling and simulation of power electronic modules with microchannel coolers for thermo-mechanical performance, Microelectron. Reliab. 54 (2014) 2824–2835.
[12] W. Chenniki, I. Bord-Majek, M. Louarn, V. Gaud, J.-L. Diot, K. Wongtimnoi, Y. Ousten, Liquid crystal polymer for QFN packaging: predicted thermo-mechanical fatigue and design for reliability, Microelectron. Reliab. 55 (12) (2015) 2793–2798.
[13] I. Gershman, J.B. Bernstein, Structural health monitoring of solder joints in QFN package, Microelectron. Reliab. 52 (12) (2012) 3011–3016.
[14] D.G. Yang, K.M.B. Jansen, L.J. Ernst, G.Q. Zhang, W.D. van Driel, H.J.L. Bressers, J.H.J. Janssen, Numerical modeling of warpage induced in QFN array molding process, Microelectron. Reliab. 47 (2–3) (2007) 310–318.
[15] A. Baïri, Thermal design of tilted electronic assembly with active QFN16 package subjected to natural convection, Int. Commun. Heat Mass Transfer 66 (2015) 240–245.
[16] A. Baïri, O. Haddad, Detailed correlations on natural convective heat transfer coefficients for QFN32 electronic device on inclined PCB, Numer. Heat Transfer, Part A 69 (8) (2016) 841–849, http://dx.doi.org/10.1080/10407782.2015.1090850.
[17] A. Baïri, Free convective heat transfer coefficient for high powered and tilted QFN64 electronic device, Microelectron. Reliab. 66 (2016) 85–91.
[18] A. Baïri, Correlations highlighting effects of the PCB's copper ratio on the free convective heat transfer for a tilted QFN32 electronic package, Int. J. Heat Mass Transf. 92 (2016) 110–119.
[19] A. Baïri, C. Ortega Hermoso, D. San Martín Ortega, O. Haddad, Echanges convectifs naturels pour les montages électroniques inclinés équipés de QFN64, Proceedings of the French Thermal Congress 2016 (Congrès Français de Thermique 2016, Thermique et Multiphysique), Toulouse, France, May 31–June 3, 2016.
[20] O. Souhar, C. Prud'homme, Numerical analysis method of heat transfer in an electronic component using sensitivity analysis, J. Comput. Electron. 13 (4) (2014) 1042–1053.
[21] D. Vasileska, K. Raleva, S.M. Goodnick, Modeling heating effects in nanoscale devices: the present and the future, J. Comput. Electron. 7 (2) (2008) 66–93.
[22] A. Baïri, C. Ortega Hermoso, D. San Martín Ortega, Effects of the molding compound's thermal conductivity on the thermal state of the QFN64 electronic package subjected to natural convection, 12th International Conference on Heat Transfer Fluid Mechanics and Thermodynamics, HEFAT 2016, Malaga (Spain), 11–13 July 2016.
[23] http://www.amkor.com.
[24] Hot Disk TPS 2500 S http://www.hotdiskinstruments.com/
[25] A. Maqsood, N. Amin, M. Maqsood, G. Shabbir, A. Mahmood, S.E. Gustafsson, Simultaneous measurements of thermal conductivity and thermal diffusivity of insulators, fluids and conductors using the transient plane source (TPS) technique, Int. J. Energy Res. 18 (9) (1994) 777–782.
[26] T. Ishizaki, M. Yanase, A. Kuno, T. Satoh, M. Usui, F. Osawa, Y. Yamada, Thermal simulation of joints with high thermal conductivities for power electronic devices, Microelectron. Reliab. 55 (2015) 1060–1066.
[27] http://www.movimed.com/Cameras_FLIR.htm#A40.

Please cite this article as: A. Baïri, et al., Thermal state of electronic assemblies applied to smart building equipped with QFN64 device subjected to natural convection, Microelectronics Reliability (2017), http://dx.doi.org/10.1016/j.microrel.2017.01.002